

Circulating tumor DNA as a liquid biopsy in plasma cell dyscrasias

Bernhard Gerber,¹ Martina Manzoni,² Valeria Spina,³ Alessio Bruscazzin,³ Marta Lionetti,² Sonia Fabris,⁴ Marzia Barbieri,⁴ Gabriella Ciceri,² Alessandra Pompa,⁴ Gabriela Forestieri,³ Erika Lerch,⁵ Paolo Servida,⁵ Francesco Bertoni,³ Emanuele Zucca,⁵ Michele Ghielmini,⁵ Agostino Cortelezzi,^{2,4} Franco Cavalli,^{3,5} Georg Stussi,¹ Luca Baldini,^{2,4} Davide Rossi^{1,3} and Antonino Neri^{2,4}

¹Division of Hematology, Oncology Institute of Southern Switzerland, Bellinzona, Switzerland; ²Department of Oncology and Hemato-oncology, University of Milan, Italy; ³Institute of Oncology Research, Oncology Institute of Southern Switzerland, Bellinzona, Switzerland; ⁴Hematology Unit, Foundation IRCCS Ca' Granda Ospedale Maggiore Policlinico, Milan, Italy and ⁵Division of Oncology, Oncology Institute of Southern Switzerland, Bellinzona, Switzerland.

BG and MM contributed equally to this work

*Correspondence: antonino.neri@unimi.it/davide.rossi@eoc.ch
doi:10.3324/haematol.2017.184358*

SUPPLEMENTARY MATERIAL

Circulating tumor DNA as a liquid biopsy in plasma cell dyscrasias

Bernhard Gerber,¹ Martina Manzoni,² Valeria Spina,³ Alessio Brusca, ³ Marta Lionetti,² Sonia Fabris,⁴ Marzia Barbieri,⁴ Gabriella Ciceri,² Alessandra Pompa,⁴ Gabriela Forestieri,³ Erika Lerch,⁵ Paolo Servida,⁵ Francesco Bertoni,³ Emanuele Zucca,⁵ Michele Ghielmini,⁵ Agostino Cortelezzi,^{2,4} Franco Cavalli,^{3,5} Georg Stussi,¹ Luca Baldini,^{2,4} Davide Rossi^{1,3} and Antonino Neri^{2,4}

¹Division of Hematology, Oncology Institute of Southern Switzerland, Bellinzona, Switzerland;

²Department of Oncology and Hemato-oncology, University of Milano, Italy;

³Institute of Oncology Research, Oncology Institute of Southern Switzerland, Bellinzona, Switzerland;

⁴Hematology Unit, Foundation IRCCS Ca' Granda Ospedale Maggiore Policlinico, Milan, Italy;

⁵Division of Oncology, Oncology Institute of Southern Switzerland, Bellinzona, Switzerland.

BG and MM contributed equally to this work

Supplementary Methods	page 3
Supplementary Table S1	page 5
Supplementary Table S2	page 6
Supplementary Table S3	page 9
Supplementary Figure S1	page 11
Supplementary Figure S2	page 12
Supplementary Figure S3	page 13
Supplementary Figure S4	page 14
Supplementary Figure S5	page 15

Supplementary Methods

Patients

The study had a prospective, observational, nonintervention design and consisted in the collection of peripheral blood (PB) samples and clinical data from plasma cell (PC) dyscrasia patients. Inclusion criteria were: (1) male or female adults ≥ 18 years old; (2) diagnosis of multiple myeloma (MM) or monoclonal gammopathy of undetermined significance (MGUS) after pathological revision; (3) evidence of signed informed consent. A total of 28 patients fulfilled the inclusion criteria and were recruited for the study from September 2016 to May 2017 (Supplementary Table S1). The following biological material was collected: (1) cfDNA isolated from plasma, (2) tumor genomic DNA (gDNA) from the CD138+ purified PCs from BM aspiration, for comparative purposes, and (3) normal germline gDNA extracted from peripheral blood (PB) granulocytes after Ficoll separation. Patients provided informed consent in accordance with local institutional review board requirements and the Declaration of Helsinki.

Isolation and analysis of plasma cfDNA

PB (20 ml maximum) was collected in Cell-Free DNA BCT tubes that allow obtaining stable cfDNA samples while preventing gDNA contamination that may occur due to nucleated cell disruption during sample storage, thus avoiding pre-analytical issues affecting cfDNA genotyping. PB was centrifuged at 820 g for 10 min to separate plasma from cells. Plasma was then further centrifuged at 20000 g for 10 min to pellet and remove any remaining cells and stored at -80°C until DNA extraction. cfDNA was extracted from 1-3 ml aliquots of plasma (to allow the recovery of enough genomic equivalents of DNA to reach a genotyping sensitivity of 10^{-3}) using the QIAamp circulating nucleic acid kit (Qiagen) and quantized using Quant-iT™ PicoGreen dsDNA Assay kit (ThermoFisher Scientific). Contamination of plasma cfDNA from gDNA released by blood nucleated cell disruption was ruled out by checking, through the Bioanalyzer (Agilent Technologies) instrument, the size of the DNA extracted from plasma.

gDNA extraction

PB granulocytes were separated by Ficoll gradient density centrifugation as a source of normal germline gDNA. Tumor gDNA was isolated from PCs purified using CD138 immunomagnetic microbeads as previously described^{1,2} (CD138+ cell percentage was $\geq 90\%$ in all cases). gDNA was extracted according to standard procedures.

Library design for hybrid selection

A targeted resequencing gene panel, including coding exons and splice sites of 14 genes that are recurrently mutated in MM patients, was specifically designed for this project (target region: 30989bp: *BRAF*, *CCND1*, *CYLD*, *DIS3*, *EGR1*, *FAM46C*, *IRF4*, *KRAS*, *NRAS*, *PRDM1*, *SP140*, *TP53*, *TRAF3*, *ZNF462*; Supplementary Table S2). Inclusion criteria of gene panel design were based on publicly available sequencing data from three distinct datasets³⁻⁵ and were as follows: (i) genes that were recurrently mutated in $\geq 3\%$ of MM tumors; (ii) genes that were cross-validated in at least two of the considered genomic datasets. An *in silico* validation of the designed gene panel in the three aforementioned patients cohorts resulted in the recovery of at least one clonal mutation in 68% (95% confidence interval [CI]: 58 to 76) of MM cases.

CAPP-seq library preparation and ultra-deep NGS

The gene panel was analyzed in plasma cfDNA, and for comparative purposes to filter out polymorphisms, in normal gDNA from the paired granulocytes as source of germline material. The gDNA from the paired CD138+ purified plasma cells from BM aspiration was also investigated in the same cases to assess the accuracy of plasma cfDNA genotyping. Tumor and germline gDNA (median 400 ng) were sheared through sonication before library construction to obtain 200-bp fragments. Plasma cfDNA, which is naturally fragmented, was used (average: 59 ng; median: 48 ng; range: 0.05-400 ng) for library construction without additional fragmentation. Targeted ultra-deep-next generation sequencing was performed on plasma cfDNA, tumor and germline gDNA by using the CAPP-seq approach, which has been validated for plasma cfDNA genotyping⁶. The NGS libraries were constructed using the KAPA Library Preparation Kit (Kapa Biosystems) and hybrid selection was performed with the custom SeqCap EZ Choice Library (Roche NimbleGen). The manufacturer's protocols were modified as previously reported⁶. Multiplexed libraries were sequenced using 300-bp paired-end runs on an Illumina MiSeq sequencer. Each run included 24 multiplexed samples in order to allow >2000x coverage in >80% of the target region.

Bioinformatic pipeline for variant calling

Mutation calling in plasma cfDNA was performed separately and in blind from mutation calling in tumor gDNA from purified PCs. We deduped FASTQ sequencing reads by utilizing FastUniq v1.1. The deduped FASTQ sequencing reads were locally aligned to the hg19 version of the human genome using BWA v.0.6.2, and sorted, indexed and assembled into a mpileup file using SAMtools v.1. The aligned reads were processed with mpileup. Single nucleotide variations and indels were called in plasma cfDNA vs normal gDNA, and tumor gDNA vs normal gDNA, respectively, by using the somatic function of VarScan2 (a minimum Phred quality score of 30 was imposed). The variant called by VarScan 2 were annotated by using SeattleSeq Annotation 138. Variants annotated as SNPs, intronic variants mapping >2 bp before the start or after the end of coding exons, and synonymous variants were filtered out. To filter out variants below the base-pair resolution background frequencies, the Fisher's exact test was used to test whether the variant frequency called by VarScan 2 in cfDNA or tumor gDNA, respectively, was significantly higher from that called in the corresponding paired germline gDNA, after adjusting for multiple comparison by Bonferroni test (Bonferroni-adjusted $P=4.03252e-7$). To further filter out systemic sequencing errors, a database containing all background allele frequencies in all the specimens analyzed was assembled. Based on the assumption that all background allele fractions follow a normal distribution, a Z-test was employed to test whether a given variant differs significantly in its frequency from typical DNA background at the same position in all the other DNA samples, after adjusting for multiple comparison by Bonferroni. Variants that did not pass this filter were not further considered. Variant allele frequencies for the resulting candidate mutations and the background error rate were visualized using IGV (see Supplementary Figure S5 for a representative example).

Statistical analysis

The sensitivity and specificity of plasma cfDNA genotyping were calculated in comparison with tumor gDNA genotyping as the gold standard. The analysis were performed with the Statistical Package for the Social Sciences (SPSS) software (Chicago, IL) and with R statistical package (<http://www.r-project.org>).

Supplementary Table S1. Patients' characteristics

ID	Age	Gender	Diagnosis	Phase	% of PCs in BM biopsy	Monoclonal component	FLC ratio	ISS stage	del(13q)	del(17p)	t(4;14)	t(14;16)	t(11;14)	HD	1p loss	1q gain
1	46	F	MM	ND	50	Micromolecular λ	λ/κ FLC = 753	3	neg	neg	neg	neg	pos	neg	neg	neg
2	52	M	MM	ND	90	IgG κ	κ/λ FLC = 708	3	pos	neg	neg	neg	neg	pos	neg	pos
3	70	M	MM	ND	30	IgG κ	κ/λ FLC = 104	1	neg	pos	neg	neg	neg	pos	neg	neg
4	53	M	MM	RR	25	IgA κ	κ/λ FLC = 3	2	n.d.	n.d.	n.d.	n.d.	n.d.	pos	neg	pos
5	56	M	MM	ND	80	IgG κ	κ/λ FLC = 36	3	neg	neg	neg	neg	neg	neg	pos	pos
6	66	M	MM	ND	28	IgA λ	λ/κ FLC = 182	1	neg	neg	neg	neg	neg	pos	neg	pos
7	46	F	MM	RR	30	Micromolecular λ	λ/κ FLC > 27000	1	pos	neg	neg	neg	neg	pos	neg	pos
8	52	F	MM	ND	45	Micromolecular λ	λ/κ FLC = 446	1	pos	neg	neg	neg	neg	pos	neg	pos
9	76	M	sMM	ND	55	IgG κ	κ/λ FLC = 4	n.a.	neg	neg	neg	neg	neg	pos	neg	pos
10	76	F	MM	ND	30	IgA λ	λ/κ FLC = 6	1	n.d.	neg	neg	neg	neg	neg	neg	pos
11	54	M	MM	ND	40	IgA κ	κ/λ FLC = 19	2	pos	neg	neg	neg	neg	pos	neg	neg
12	77	M	MM	ND	30	IgG κ	κ/λ FLC = 17	2	neg	neg	neg	neg	neg	pos	neg	neg
13	64	M	MM	ND	60	IgA λ	λ/κ FLC = 210	3	n.d.	neg	neg	neg	neg	neg	neg	pos
14	61	F	sMM	ND	55	IgG κ	κ/λ FLC = 29	n.a.	pos	neg	neg	neg	neg	pos	neg	neg
15	68	M	MM	ND	70	IgA λ	λ/κ FLC = 65	3	pos	pos	pos	neg	neg	neg	neg	pos
16	76	F	sMM	ND	18	IgG κ	κ/λ FLC = 44	n.a.	n.d.	neg	neg	neg	neg	pos	neg	neg
17	59	M	MM	ND	90	Micromolecular λ	λ/κ FLC = 129	3	pos	pos	neg	neg	pos	pos	pos	neg
18	68	F	MM	ND	40	IgG λ	λ/κ FLC = 338	1	n.d.	neg	neg	neg	neg	neg	neg	pos
19	64	F	MM	RR	65	IgG κ	κ/λ FLC = 15	2	neg	neg	neg	neg	pos	neg	neg	neg
20	82	F	MM	ND	11	IgG κ	κ/λ FLC = 21	1	n.d.	neg	neg	neg	pos	neg	neg	neg
21	59	F	sMM	ND	10	IgG λ	λ/κ FLC = 5	n.a.	n.d.	neg	neg	neg	pos	neg	neg	neg
22	78	M	MGUS	ND	8	IgM κ	κ/λ FLC = 3	n.a.	neg	neg	neg	neg	pos	neg	neg	neg
26	47	F	MM	ND	50	IgA λ	λ/κ FLC = 6	1	n.d.	neg	neg	neg	neg	neg	neg	neg
27	71	M	MM	ND	28	IgG κ	κ/λ FLC = 109	1	n.d.	neg	neg	neg	neg	neg	neg	pos
28	68	M	sMM	ND	38	IgA λ	λ/κ FLC = 23	n.a.	n.d.	neg	neg	neg	neg	pos	neg	neg
29	69	M	MM	ND	70	IgG κ	κ/λ FLC = 200	2	n.d.	neg	neg	neg	neg	neg	neg	pos
30	50	F	MM	ND	60	IgA κ	κ/λ FLC = 108	1	n.d.	neg	neg	neg	neg	neg	neg	neg
31	61	F	MGUS	ND	7	IgG κ	κ/λ FLC = 4	n.a.	neg	neg	neg	neg	neg	pos	neg	neg

Abbreviations: F, female; M, male; MM, multiple myeloma; sMM, smoldering multiple myeloma; MGUS, monoclonal gammopathy of undetermined significance; ND, newly diagnosed; RR, relapsed/refractory; BM, bone marrow; FLC, free light-chain; ISS, International Staging System; n.a., not applicable; n.d., not determined; HD, hyperdiploidy.

Supplementary Table S2. Target region

<i>Gene</i>	<i>chromosome</i>	<i>coding exon start plus splice site (2bp)</i>	<i>coding exon stop plus splice site (2bp)</i>
<i>NRAS</i>	chr1	115251156	115251277
		115252188	115252351
		115256419	115256601
		115258669	115258783
<i>FAM46C</i>	chr1	118165491	118166666
<i>CCND1</i>	chr11	69456082	69456281
		69457797	69458016
		69458598	69458761
		69462760	69462912
<i>KRAS</i>	chr12	69465884	69466050
		25368375	25368496
		25378546	25378709
		25380166	25380348
<i>DIS3</i>	chr13	25398206	25398318
		73333933	73334018
		73334665	73334791
		73335499	73335661
		73335782	73335954
		73336059	73336277
		73337587	73337747
		73340108	73340198
		73342921	73343052
		73345040	73345128
		73345217	73345285
		73345931	73346036
		73346295	73346415
		73346829	73346979
73347820	73347961		
73348082	73348199		
73349347	73349515		
73350061	73350232		
73351556	73351633		
73352323	73352520		
73354982	73355143		
73355741	73355970		
<i>TRAF3</i>	chr14	103336537	103336785
		103338252	103338307
		103341959	103342067
		103342693	103342864
		103352524	103352608
		103355895	103355973
		103357660	103357756
		103363596	103363740
		103369590	103369768
		103371548	103372121
<i>CYLD</i>	chr16	50783610	50784115
		50785513	50785819
		50788228	50788337
		50810088	50810190
		50811734	50811854
		50813574	50813957
		50815155	50815324
		50816234	50816379
		50818238	50818364
		50820764	50820859
		50821695	50821765
		50825467	50825603
		50826506	50826618
50827455	50827577		
50828121	50828341		
50830233	50830419		

Supplementary Table S2. (continued)

<i>Gene</i>	<i>chromosome</i>	<i>coding exon start plus splice site (2bp)</i>	<i>coding exon stop plus splice site (2bp)</i>
<i>TP53</i>	chr17	7572927	7573010
		7573925	7574035
		7576851	7576928
		7577017	7577157
		7577497	7577610
		7578175	7578291
		7578369	7578556
		7579310	7579592
		7579698	7579723
		7579837	7579912
<i>SP140</i>	chr2	231090560	231090620
		231101796	231101977
		231102926	231103098
		231106117	231106204
		231108444	231108528
		231109701	231109797
		231110576	231110657
		231112629	231112782
		231113598	231113685
		231115694	231115778
		231118029	231118134
		231120165	231120249
		231134245	231134335
		231134550	231134670
		231135299	231135356
		231149059	231149128
		231150465	231150549
		231152605	231152683
		231155173	231155281
		231157359	231157505
231158984	231159035		
231162134	231162179		
231174637	231174756		
231175456	231175568		
231175867	231175948		
231176165	231176312		
231177299	231177399		
<i>EGR1</i>	chr5	137801451	137801759
		137802444	137803770
<i>IRF4</i>	chr6	393153	393370
		394819	395009
		395845	395937
		397106	397254
		398826	398937
		401422	401779
		405016	405132
407453	407598		
<i>PRDM1</i>	chr6	106534429	106534472
		106536074	106536326
		106543488	106543611
		106547173	106547429
		106552698	106553810
		106554244	106554376
		106554784	106555361

Supplementary Table S2. (continued)

<i>Gene</i>	<i>chromosome</i>	<i>coding exon start plus splice site (2bp)</i>	<i>coding exon stop plus splice site (2bp)</i>
<i>BRAF</i>	chr7	140434397	140434572
		140439610	140439748
		140449085	140449220
		140453073	140453195
		140453985	140454035
		140476710	140476890
		140477789	140477877
		140481374	140481495
		140482819	140482959
		140487346	140487386
		140494106	140494269
		140500160	140500283
		140501210	140501362
		140507758	140507864
		140508690	140508797
		140534407	140534674
		140549909	140550014
		140624364	140624503
<i>ZNF462</i>	chr9	109685665	109685886
		109686412	109692042
		109692804	109692972
		109694725	109694832
		109697782	109697904
		109701195	109701390
		109734284	109734555
		109736416	109736556
		109746465	109746692
		109765573	109765709
		109771824	109771951
		109773102	109773311

Absolute chromosome coordinates are based on the hg19 version of the human genome assembly.

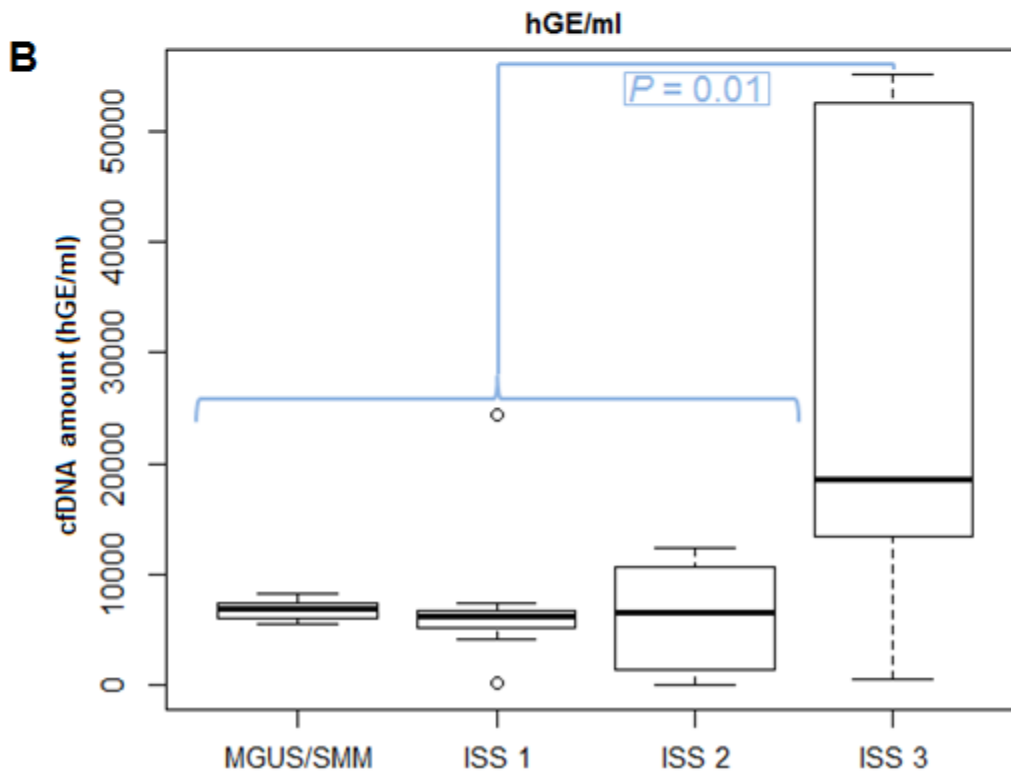
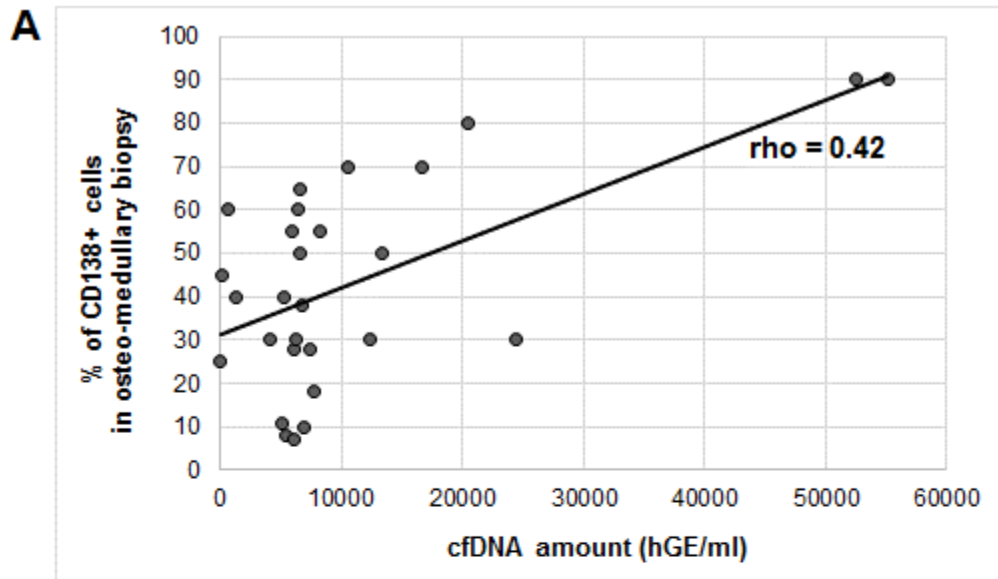
Supplementary Table S3. Percentage of target region covered $\geq 1000X$ and $\geq 2000X$ in distinct patient samples.

<i>ID</i>	<i>Sample</i>	<i>Target Region Coverage (%)</i>	
		$\geq 1000X$	$\geq 2000X$
ID1	GL	100.0	99.5
	PCS	99.6	98.3
	PL	99.4	97.9
ID2	GL	99.5	99.5
	PCS	99.4	96.9
	PL	97.8	83.5
ID3	GL	98.7	85.9
	PCS	99.9	99.5
	PL	98.9	95.8
ID4	GL	98.3	43.0
	PCS	100.0	100.0
	PL	97.6	58.5
ID5	GL	97.7	63.4
	PCS	100.0	99.6
	PL	98.2	93.3
ID6	GL	100.0	99.5
	PCS	99.5	99.5
	PL	99.4	97.4
ID7	GL	99.6	99.5
	PCS	99.6	98.8
	PL	99.5	97.9
ID8	GL	99.5	98.6
	PCS	99.5	99.5
	PL	98.6	91.9
ID9	GL	99.5	98.8
	PCS	99.5	98.9
	PL	99.4	97.8
ID10	GL	99.5	99.0
	PCS	99.3	96.9
	PL	99.5	98.5
ID11	GL	99.5	98.7
	PCS	99.5	99.3
	PL	99.3	95.5
ID12	GL	99.5	99.0
	PCS	99.5	99.1
	PL	94.5	21.9
ID13	GL	99.5	98.9
	PCS	99.5	98.7
	PL	98.7	86.0
ID14	GL	99.5	98.8
	PCS	99.6	98.8
	PL	99.4	96.5

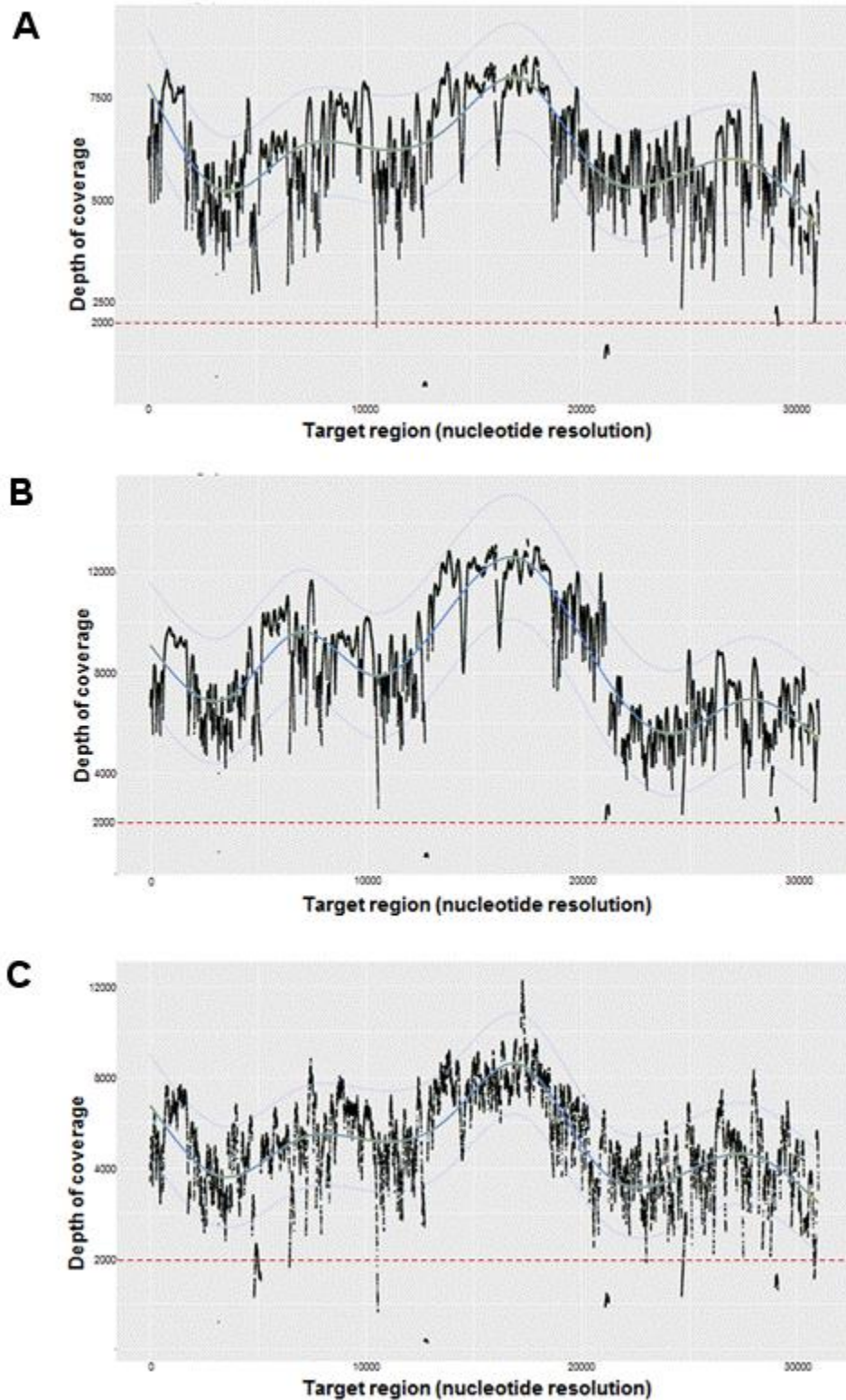
Supplementary Table S3. (continued)

ID	Sample	Target Region Coverage (%)	
		$\geq 1000X$	$\geq 2000X$
ID15	GL	99.5	98.7
	PCS	99.5	98.6
	PL	99.4	98.0
ID16	GL	99.5	98.9
	PCS	99.5	98.3
	PL	97.3	62.8
ID17	GL	98.6	97.5
	PCS	99.5	95.2
	PL	98.5	97.0
ID18	GL	98.7	96.3
	PCS	94.7	84.0
	PL	98.7	97.8
ID19	GL	98.4	92.0
	PCS	96.4	74.9
	PL	98.7	97.5
ID20	GL	98.6	96.5
	PCS	97.7	95.2
	PL	98.7	96.8
ID21	GL	98.5	94.9
	PCS	98.0	94.9
	PL	98.6	96.7
ID22	GL	98.7	97.5
	PCS	98.7	97.8
	PL	98.7	96.5
ID26	GL	98.9	98.2
	PCS	99.5	99.5
	PL	99.4	97.1
ID27	GL	99.5	99.0
	PCS	99.5	98.8
	PL	99.5	98.8
ID28	GL	99.5	99.0
	PCS	99.5	99.5
	PL	98.7	90.3
ID29	GL	98.2	94.5
	PCS	99.6	99.5
	PL	99.6	99.4
ID30	GL	99.5	98.9
	PCS	100.0	99.5
	PL	99.5	98.1
ID31	GL	99.6	98.9
	PCS	99.6	98.9
	PL	99.4	98.3

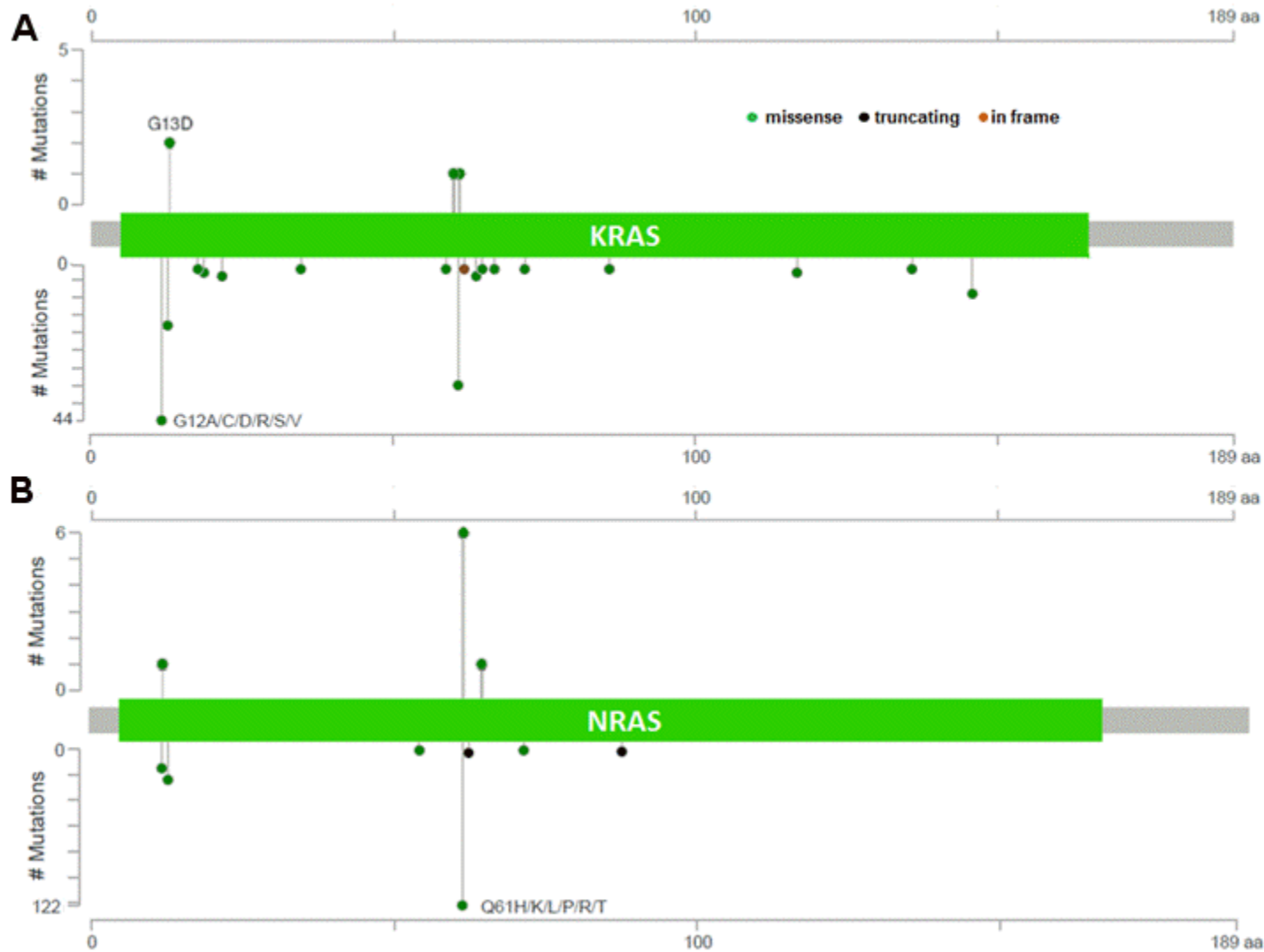
Abbreviations: GL, normal germline DNA from granulocytes; PCS, tumor genomic DNA from plasma cells; PL, cfDNA from plasma.



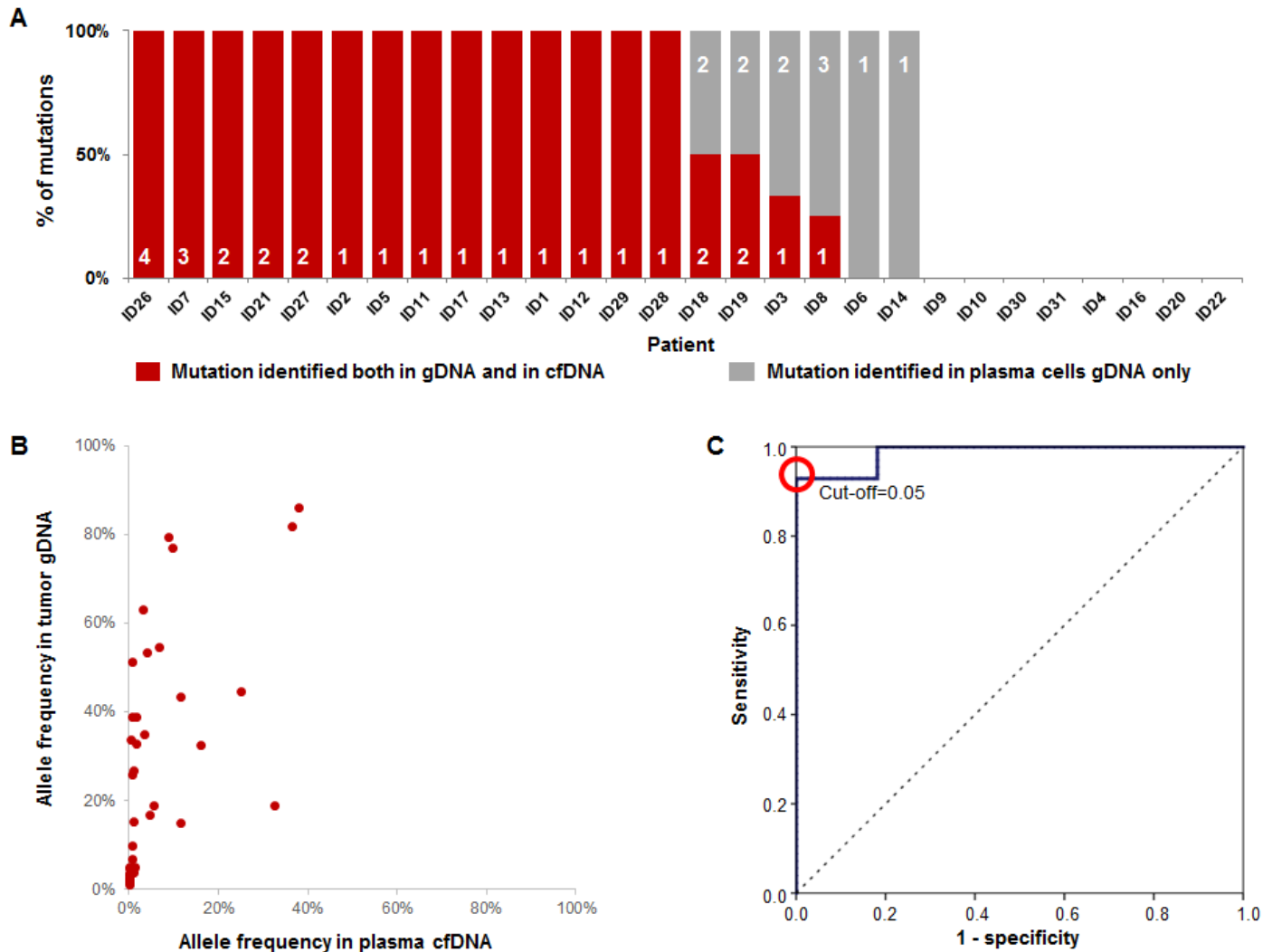
Supplementary Figure S1. (A) Correlation between cfDNA amount and bone marrow plasma cell infiltration. **(B)** cfDNA amount according to diagnosis/risk stratification: the levels of cfDNA are significantly higher in MM patients at ISS stage 3 compared with MGUS/SMM samples and MM cases at ISS stages 1-2 ($P=0.01$; Mann-Whitney test).



Supplementary Figure S2. Coverage across the target region. Depth of coverage (y axis) across the target region (x axis) by CAPP-seq of **(A)** gDNA from the germline (granulocytes) samples, **(B)** tumor gDNA from bone marrow plasma cells, and **(C)** plasma cfDNA. Each dot represents the sequencing depth on that specific position of the target region of one single individual sample. The solid blue line shows the median depth of coverage, while the dash blue lines show the interquartile range. The dashed red line shows the 2000X coverage.

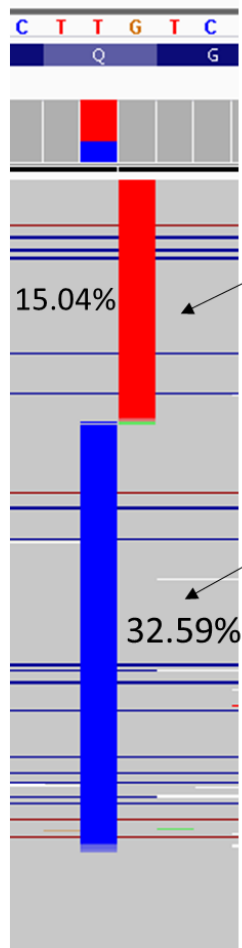


Supplementary Figure S3. Prevalence and molecular spectrum of nonsynonymous somatic mutations discovered in plasma cfDNA. The most mutated genes are reported: **(A)** *KRAS* gene and **(B)** *NRAS* gene. The molecular spectrum of nonsynonymous somatic mutations identified in plasma cfDNA (in the upper part of the figure) compared with the molecular spectrum of nonsynonymous somatic mutations that have been detected in the tumor gDNA in published MM series and reported in the COSMIC database (version 81)⁷ (in the lower part of the figure). Mutation maps were obtained through Mutation Mapper version 1.0.1. Color codes indicate the type of the mutations: truncating mutations include nonsense, frameshift deletion, frameshift insertion, splice site.



Supplementary Figure S4. Concordance between plasma cfDNA and tumor gDNA genotyping. **(A)** The fraction of tumor biopsy–confirmed mutations that were detected in plasma is shown. Patients are ordered by decreasing detection rates. The red portion of the bars indicates the prevalence of tumor biopsy–confirmed mutations that were detected in plasma cfDNA. The gray portion of the bars indicates the prevalence of tumor biopsy–confirmed mutations that were not detected in plasma cfDNA. **(B)** The mutation abundance in plasma cfDNA vs the mutation abundance in tumor gDNA is comparatively represented in the scatter plot for each identified variant. **(C)** ROC analysis illustrating the performance of gDNA genotyping in discriminating the ability of cfDNA genotyping to detect biopsy–confirmed mutations according to the variant allele frequency of mutations in tumor gDNA.

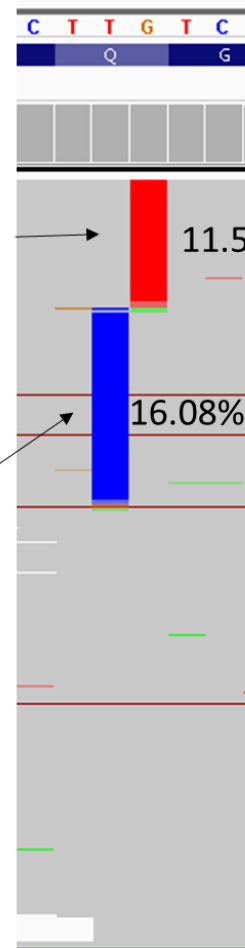
A) ID26 bone marrow



NRAS p.Q61K
g.chr1:115256530G>T

NRAS p.Q61R
g.chr1:115256529T>C

B) ID26 cfDNA



Supplementary Figure S5. Visualization of deep sequencing data in BM gDNA (A) and cfDNA (B) of patient ID26 by Integrated Genome Viewer software. Two adjacent base substitutions affecting the same codon and originating distinct *NRAS* p.Q61R and p.Q61K mutations are shown. The lack of sequencing reads carrying both mutations suggested that these two substitutions likely involved different tumor subclones. Reads were sorted by base at chr1:115,256,529 locus and then again sorted by base at chr1:115,256,530 locus. Red bars show G>T substitutions at the chr1:115,256,530 locus. Blue bars show T>C substitution at the chr1:115,256,529 locus.

References

1. Fabris S, Agnelli L, Mattioli M, et al. Characterization of oncogene dysregulation in multiple myeloma by combined FISH and DNA microarray analyses. *Genes, chromosomes & cancer*. 2005;42(2):117-27.
2. Mattioli M, Agnelli L, Fabris S, et al. Gene expression profiling of plasma cell dyscrasias reveals molecular patterns associated with distinct IGH translocations in multiple myeloma. *Oncogene*. 2005;24(15):2461-73.
3. Bolli N, Avet-Loiseau H, Wedge DC, et al. Heterogeneity of genomic evolution and mutational profiles in multiple myeloma. *Nature communications*. 2014;5:2997.
4. Kortuem KM, Braggio E, Bruins L, et al. Panel sequencing for clinically oriented variant screening and copy number detection in 142 untreated multiple myeloma patients. *Blood Cancer J*. 2016;6:e397.
5. Lohr JG, Stojanov P, Carter SL, et al. Widespread genetic heterogeneity in multiple myeloma: implications for targeted therapy. *Cancer Cell*. 2014;25(1):91-101.
6. Newman AM, Bratman SV, To J, et al. An ultrasensitive method for quantitating circulating tumor DNA with broad patient coverage. *Nature medicine*. 2014;20(5):548-54.
7. Forbes SA, Beare D, Boutselakis H, et al. COSMIC: somatic cancer genetics at high-resolution. *Nucleic acids research*. 2017;45(D1):D777-D83.